Research Square

Preprints are preliminary reports that have not undergone peer review.
They should not be considered conclusive, used to inform clinical practice,
or referenced by the media as validated information.

Modeling water productivity and water footprint of drip irrigated rice in a Mediterranean environment

Itzel Inti Donati
CREA- PB, Research Centre for Agricultural Policies and Bioeconomy
Pasquale Garofalo
CREA-AA , Council for Agricultural Research and Economics Agriculture and Environment Research Center
Andrea Martelli
CREA- PB, Research Centre for Agricultural Policies and Bioeconomy
Davide Rapinesi
CREA- PB, Research Centre for Agricultural Policies and Bioeconomy
Stefano Monaco
CREA - IT, Research Centre for Engineering and Agro-food processing
Leonardo Verdi
University of Florence DAGRI,Department of Agriculture, Food, Environment and Forestry
Anna Dalla Marta
University of Florence DAGRI,Department of Agriculture, Food, Environment and Forestry
Filiberto Altobelli
filiberto.altobelli@crea.gov.it

CREA- PB, Research Centre for Agricultural Policies and Bioeconomy

Research Article

Keywords: water management, deficit irrigation, climate resilient crops, irrigated rice

Posted Date: May 20th, 2026

DOI: https://doi.org/10.21203/rs.3.rs-9497634/v1

License: This work is licensed under a Creative Commons Attribution 4.0 International License.
Read Full License

Additional Declarations: No competing interests reported.

Abstract

Rice cultivation in Mediterranean environments is increasingly constrained by declining water availability, challenging the sustainability of traditional flooded irrigation systems. This study aimed to calibrate and validate the FAO AquaCrop model for rice (Oryza sativa L.) grown under drip irrigation and to assess crop water productivity and water footprint components under non-flooded conditions. Field experiments were conducted over three consecutive growing seasons (2021–2023) in Tuscany (central Italy), characterized by contrasting climatic conditions. AquaCrop was calibrated and validated using observed data on canopy cover, aboveground biomass, soil water content, and grain yield. Model results closely aligned with experimental observations, with satisfactory statistical indicators for canopy development, biomass accumulation, and yield across years. Simulated and observed yields ranged from approximately 2.7 to 4.0 t ha^{-1}, demonstrating that drip irrigation can sustain stable rice production under water-limited conditions. Water footprint analysis revealed a substantial reduction in blue water consumption compared with conventional flooded systems, with irrigation volumes consistently below 7,000 m^3 ha^{-1} and total water footprint decreasing from 2,182 to 1,603 m^3 t^{-1} over the study period. These results highlight the potential of drip irrigation, supported by crop modeling, to improve water use efficiency and reduce freshwater pressure while maintaining acceptable rice yields in Mediterranean environments.

1. Introduction

Rice (*Oryza sativa* L.) is one of the most important staple crops worldwide and plays a central role in food security. In Europe, Italy is the leading rice producer, where cultivation has traditionally relied on continuously flooded systems, particularly in northern regions (Arcieri & Ghinassi, 2020). Rice is also grown in marginal and climatically sensitive areas of central Italy, where water availability is increasingly constrained and traditional irrigation practices are becoming more difficult to sustain.

Flooded rice cultivation has historically ensured stable yields due to continuous water supply, effective weed control, and favorable nutrient dynamics (Bouman et al., 2007; Datta et al., 2017). However, this production system is characterized by very high-water requirements, with seasonal irrigation volumes ranging from 13,000 to more than 60,000 m^3 ha^{-1} under Italian conditions (Arcieri & Ghinassi, 2020). Declining freshwater availability for agriculture, combined with rising temperatures and increasing climate variability, raises concerns about the long-term sustainability of permanently flooded rice systems, particularly in Mediterranean environments.

In response to these challenges, increasing attention has been directed toward alternative water-saving irrigation strategies, including dry seeding, alternate wetting and drying, and aerobic rice systems (Bouman et al., 2007; Ranghetti & Boschetti, 2022). Among these approaches, micro-irrigation techniques such as drip irrigation have shown considerable potential to reduce irrigation water use while maintaining high yield levels. The optimisation of irrigation practices has become a priority to ensure sustainable water management in agriculture and is necessary to assess its potential for improving

water use efficiency (Altobelli et al., 2018; Martelli et al., 2025). Recent studies have reported water savings exceeding 40–50% compared with conventional flooding, highlighting the opportunity to substantially improve water-use efficiency in rice-based systems (Sasmita et al., 2022; Mallareddy et al., 2023). Beyond total water use, the assessment of irrigation sustainability requires indicators capable of capturing both the quantity and origin of water resources involved. The water footprint (WF) framework provides a comprehensive approach by distinguishing between green water (effective rainfall), blue water (surface and groundwater used for irrigation), and grey water (associated with pollutant loads) (Chapagain & Hoekstra, 2011). Rice cultivation is generally associated with high WF values, largely due to its strong dependence on blue water under flooded conditions, making WF analysis particularly relevant when evaluating alternative irrigation strategies (Chapagain & Hoekstra, 2011; Mekonnen & Hoekstra, 2011).

To evaluate these strategies effectively, crop growth models represent valuable tools for supporting the assessment and optimization of irrigation management under changing climatic conditions. Among these, the FAO AquaCrop model has been widely applied to simulate crop growth, yield response to water, and water productivity across a range of crops and environments (Raes et al., 2009). While AquaCrop has been successfully calibrated and validated for rice under flooded and alternate wetting and drying regimes (Maniruzzaman et al., 2015; Mostafa et al., 2023), its application under micro-irrigation conditions remains limited, particularly in Mediterranean agro-climatic contexts.

Therefore, the primary objective of this study was to calibrate and validate the AquaCrop model for rice cultivated under drip irrigation in a Mediterranean environment. Using data from a three-year field experiment conducted in Tuscany (central Italy), the study aimed to assess crop water productivity and quantify the water footprint (WF) components associated with non-flooded rice cultivation. By integrating field observations with crop modeling and WF analysis, this study provides insights into the potential of drip irrigation as a sustainable alternative to traditional flooded rice systems in water-limited Mediterranean regions.

2. Materials and Methods

2.1. Experimental site

The field experiment was carried out for three years (2021, 2022, 2023) in farmers' fields at "Poggetti Vecchi", in the Tuscany region (Italy), 42°49'13.1"N 11°04'23.5"E, alt 4 m a.s.l.) (Fig. 1). The farm covers an area of 175 hectares, located in the Grosseto province of central Italy, in the locality of Barbaruta (Maremma Grossetana). This study area is situated within a complex agrarian framework (Fig. 1), shaped by hydrological processes influenced by the Ombrone River. The river serves as a critical source for the irrigation volumes required to satisfy the crop water demands of the district.

The study area features a Mediterranean climate (Köppen-Geiger class: Csa), with precipitation primarily occurring between October and March. Autumn temperatures are typically moderate, whereas the

summer period is characterized by high temperatures conditions and limited precipitation. (Macchia et al., 2013).

The climate data for the period 1991–2020, as collected by the Meteorological Service of the Italian Air Force in Grosseto (Latitude: 42.75; Longitude: 11.07; elevation: 5 m above sea level) and published by the Environmental Monitoring and Modeling Laboratory for Sustainable Development Consortium(LaMMa;https://www.lamma.toscana.it/clima-e-energia/climatologia/clima-grosseto, accessed on 19 December 2024), indicate that the average maximum annual temperature for the study area is 30.4°C, while the average minimum annual temperature is 2.7°C, and annual rainfall (average 600 mm).

Meteorological data, including daily maximum and minimum temperatures (°C), relative air humidity (%), rainfall (mm) and solar radiation (MJ m^{-2}) at daily scale during the experimental years (2021,2022,2023) were collected from a field meteorological station (µMETOS by Pessl). These data were essential for monitoring the key phenological stages, including Germination, Seedling, Flowering, Maturation, and Harvest.

Daily reference evapotranspiration (ET0i; mm) in the experimental field was calculated using the FAO Penman-Monteith equation, as outlined by (Allen et al., 2006). This calculation was based on daily measurements of solar radiation, maximum temperature (Tmax), minimum temperature (Tmin), and relative humidity (RH) recorded at the meteorological station.

Before the start of the field experiment (winter 2021), a soil analysis was carried out, revealing the chemical and physical characteristics shown in Table 1.

Table 1
Soil chemical and physical characteristics of experimental field

Factors		**Units**	**Value**
Soil texture	Clay Loam		
	Clay	%	27.5
	Silt	%	39.7
	Sand	%	32.7
	Organic matter	%	2.3
	Total Nitrogen	g kg^{-1}	1.46
	Available P	Ppm	61.4
	Total K	ppm	361.7

2.1.2. Field experiment

The rice experimental site was established on two fields, each measuring 1.5 hectares, which were divided into three replications of 450 square meters. The experiment was carried out on rice cultivated under drip irrigation, using the Caravaggio variety over a three-year period from 2021 to 2023. Sowing for the growing seasons occurred on May 17, 2021; May 12, 2022; and May 30, 2023. The experimental setup included ten reference poles arranged in two symmetrical rows, spaced 20 m apart, with 10 m between poles within each row. All positioning points were geolocated to ensure precise field mapping. Sampling of biomass and crop biophysical parameters was scheduled around each pole. Plant density was 400.00 plants m^{-2} and with row spacing of 18 cm.

Table 2

Phenological development and sowing parameters of Caravaggio Rice (2021–2023)

Phenological stages	Growing year 2021	Growing year 2022	Growing year 2023
Sowing			
Date	17/05/21	12/05/22	30/05/23
Density (kg/ha)	230	230	230
Population (plants/ha)	4000000	4000000	4000000
Plants/m²	400	400	400
Thousand Grain Weight (g)	42	42	42
Emergence			
Start	17/05/21	12/05/22	01/06/23
End	13/06/21	10/06/22	11/06/23
Tillering			
Start	13/06/21	10/06/22	12/06/23
End	08/07/21	05/07/22	07/07/23
Stem Elongation			
Start	08/07/21	05/07/22	07/07/23
End	24/07/21	22/07/22	20/07/23
Flowering			
Start	24/07/21	22/07/22	21/07/23
End	11/09/21	09/09/22	08/09/23
Onset of Senescence			
Start	11/09/21	09/09/22	08/09/23
End	15/10/21	13/10/22	10/10/23

Optimal fertilization levels were maintained throughout the growing season to prevent nutrient stress. Crop development and phenological stages were monitored during the entire crop cycle. Destructive plant tissue samples were collected from transplanting to harvest.

Collected samples were threshed, cleaned and dried to determine grain yield, which was then converted to kg ha^{-1} at 14% moisture content (Kitilu et al., 2019).

The primary yield components, including the number of fertile panicles, grain weight, moisture content, 1000-seed weight, plant height, and the number of kernels per panicle, were determined.

The length of crop cycle assured about four sampling per treatment in each year, to guarantee sufficient data to drive AquaCrop simulation model. Plants were partitioned into roots, stem, leaves and grains. The leaf area index (LAI, m^2 m^{-2}) was estimated using a ceptometer (AccuPAR, model LP-80). Measurements were conducted across the three growing seasons under varying lighting conditions and at multiple locations to ensure the collection of representative data.

The values of LAI were subsequently transformed into canopy cover (CC), which was compared with model simulated CC, using Beer's law (Ponce De León & Bailey, 2019):

$$CC = 1 - e^{(-ek\ x\ LAI_d * Cf)}$$

1

Where *ek* is the light extinction coefficient (0.75), (Rinaldi & Garofalo, 2011),*LAId* is the green leaf area and Cf is the clumping factor, calculated as:

$$Cf = 0.75 + (0.25)\ x\ \left(1 - e^{(-0.35 x LAI_d)}\right)$$

2

During the experiment, the full-water treatment by drip irrigation followed the farmer practice (FARM). The net irrigation dose (NI) for each event was determined using the FAO procedure to calculate ETc, accounting for rainfall during the period and the system distribution uniformity (DUlq) to obtain the gross irrigation dose (GI). In the experimental plots, irrigation was carried out using high-quality drip emitters designed for consistent flow despite varying pressures, with irrigation integrated when ETc reached a value of 40 mm.

2.2. The AquaCrop model and Water footprint

This study utilized the AquaCrop model, developed by the Food and Agriculture Organization (FAO), to assess rice yield, water consumption, and the WF under micro irrigation conditions. Water productivity (WP) is essential for optimizing water resources, as it encompasses various measurement dimensions, including biophysical, economic, social, and nutritional productivity, as highlighted in the literature (FAO,2022). By enhancing WP, it is possible to reduce the WF footprint associated with agricultural practices, ultimately leading to more sustainable management of water resources.

The water consumed by the crop system is measured by daily crop transpiration (Tri), which is adjusted for canopy cover (CC*) and modified by the soil water stress coefficient (KS) and crop coefficient (Kc). Daily aboveground biomass (TDM) is then calculated based on Tri and water productivity normalized for

reference evapotranspiration (WP*) (Wellens et al., 2022). Finally, dry yield (Y) is estimated at maturity using TDM and harvest index (HI).

For more detailed information on AquaCrop, readers can visit the FAO Land and Water Division website (https://www.fao.org/land-water/databases-and-software/aquacrop/en/), as well as refer to relevant publications on model calibration ((Abi Saab et al., 2015; Katerji et al., 2013).

2.3. Evaluation of Water footprint and its key components

The outcomes from CropWat were utilized to estimate the individual components of WF (m^3 t^{-1}), following the methodology outlined by Hoekstra et al. (2011):

$$WF = WFgreen + WFblue + WFgrey$$

6

For the calculation of each WF component, the crop water use (Wuse; m^3 ha^{-1}) was initially calculated for the respective components (green, blue, and grey), and their sum is the total water use ($Wuse_{tot}$).

$Wuse_{green}$ refers to the water from precipitation that is stored in the soil and is available for plant uptake. For its estimation, ETgreen was used, representing the minimum between the water requirement to meet the crop's potential ET (ETp, mm) and effective rainfall (Peff, mm). Thus, the calculation is as follows:

$$Wuse_{green} = 10* \sum_{d=1}^{lgp} ETgreen$$

7

where lgp is the duration of the crop growing period.

It should be noted that the values obtained for ETgreen and $Wuse_{green}$ were identical across all the analyzed scenarios, as they shared the same pedo-climatic context.

Consequently, there were no variations in the measured values of Peff and ETp, which resulted in consistent $Wuse_{green}$ values among the irrigation scenarios.

Following the same methodology used for $Wuse_{green}$, the value of $Wuse_{blue}$ was calculated by deriving ETblue as the minimum value between the irrigation required to meet the crop's potential water demand (IR, mm) and the effective irrigation (Ieff, mm) scheduled by AquaCrop for each simulated scenario considering a maximum daily irrigation limit of 20 mm:

$$Wuse_{blue} = 10* \sum_{d=1}^{lgp} ETblue$$

8

Grey water is defined as the amount of freshwater required to dilute pollutants to maintain water quality standards. It reflects the water needed to assimilate the pollutants generated by agricultural practices such as nitrogen fertilizer application, thereby minimizing their environmental impact. Thus, the $Wuse_{grey}$ was estimated based on the concentration of pollutants produced and the assimilative capacity of the receiving water body(Lamastra et al., 2014), calculated as:

$$Wuse_{grey} = \frac{(Nc*Fa)*\alpha}{(Cmax - Cnat)}*1000$$

9

where:

- Nc stands for N-concentration for the fertilizer (34%);
- Fa is the fertilizer amount applied in the field (150 kg ha^{-1});
- α is the nitrate leaching run-off fraction (constant) that was assumed to be equal to 0.1 (Dichio et al., 2014) [21];
- Cmax is the environmental water quality standard which was intended as the legal limit end-point of 15 mg L^{-1} (for nitrogen) as established by Italian Law Decree n. 152/2006 (MATTM, 2006)[33].
- Cnat is the natural concentration in receiving water body, generally assumed to be 0.

Finally, to determine the WF for the components outlined above, the Wuse for green, blue, and grey water corresponding to each combination of organic fertilization management x irrigation regime was divided by the respective yield. The results were then expressed in $m^3\ t^{-1}$, with the WF calculated as shown in Eq. 6.

It is important to note that since the launch of the WaPOR tool in 2019, the assessment of water use and efficiency has been enhanced, enabling large-scale evaluations of water requirements and productivity (Mahmoud et al., 2024). Nevertheless, AquaCrop offers a comprehensive crop growth model that integrates key factors, including water, soil, and management practices, to predict crop yields.

Consequently, it is particularly well-suited for detailed and crop-specific analyses, as demonstrated in the examination of rice in this study. To further explore this topic, the WaterPIP Knowledge and Action Network can be referenced. This project aims to improve access to data and information by establishing digital observatories that integrate field-level data with remote sensing techniques to monitor land and water use (https://waterpip.un-ihe.org/en).

2.2.1. Model parameterization and input

The model categorizes crop parameters into two types: conservative and non-conservative. Conservative parameters are stable and do not vary with time, location, management, or cultivar (e.g., coefficients for

canopy growth and decline, full canopy Kc, biomass water productivity, and soil water depletion thresholds). Non-conservative parameters, however, are specific to user conditions and can change significantly based on the year, location, crop variety, soil type, and climate. These include factors like sowing date and density, crop cycle length, and maximum canopy cover (Heng et al., 2009a, 2009b; Raes et al., 2009). The parameters used for model calibration and validation are outlined in Table 4. Some data were obtained from experiments carried out during the 2021, 2022, 2023 cropping seasons, while others were based on local experience or sourced from the AquaCrop reference manual as default values. Non-conservative parameters were derived from field observations of rice development and phenology, and they are calibrated using data from crops grown under optimal conditions. However, they can still be applied in stress situations through adjustment by stress response functions. Parameters tied to the specific cultivar, as well as those considered non-conservative, were subsequently modified, given that their values are dependent on the chosen cultivar and can be influenced by factors such as field management practices, soil profile characteristics, and prevailing climatic conditions.

2.2.1.1. Climatic Data inputs.

AquaCrop requires various input data, including climate data (i.e. minimum and maximum air temperatures, ETo, precipitation, and CO_2), soil data (field capacity, permanent wilting point, and saturated hydraulic conductivity), crop data (emergence date, flowering onset, flowering duration, maximum canopy cover, canopy senescence, and physiological maturity), management data (irrigation practices and field management), and initial conditions (initial soil water content) (Raes et al., 2009).

2.2.1.2. Management data inputs.

To enable AquaCrop to simulate the growth and development of processing rice in a Mediterranean climate, the crop algorithm parameters and coefficients were adjusted in two phases: calibration and validation.

The calibration phase primarily focused on the development of CC, as accurate simulation of this factor influences transpiration and ultimately the final biomass and yield of the crop. Key parameters for accurately estimating CC included the initial canopy cover (CC0), which was used to determine the corresponding plant density.

2.2.2. Model calibration and validation

To evaluate the reliability of the model, a statistical comparison was conducted between measured and simulated data, which included soil water content, dry biomass, and grain yield. The relationship between predicted and observed values was quantified using several statistical metrics: the coefficient of determination, root mean square error (RMSE), normalized root mean square error (NRMSE) (Jacovides & Kontoyiannis, 1995), Nash-Sutcliffe efficiency (EF) (Nash & Sutcliffe, 1970), and Willmott's index (d) (Willmott, 1982). These statistical parameters are detailed in Equations 3–5.

$$\mathrm{NRMSE} = \frac{1}{M}\sqrt{\sum_{i=1}^{n}\frac{(S_i - \mathrm{M}_i)^2}{n}}\, x\, 100$$

3

$$r = \frac{n\left(\sum M_i * S_i\right) - \left(\sum M_i\right)*\left(\sum MS_i\right)}{\sqrt{\left[n\sum M_i^2 - \left(\sum M_i\right)^2\right] * \left[n\sum S_i^2 - \left(\sum S_i\right)^2\right]}}$$

4

$$d = 1 - \left[\frac{\sum_{i=1}^{n}(S_i - M_i)^2}{\sqrt{\sum_{i=1}^{n}\left(\left|S_i - \bar{M}\right| + \left|M_i - \bar{M}\right|\right)^2}}\right]^2$$

5

Where *n* represents the number of observations, while *S* and *M* denote the simulated and measured values, respectively. Additionally, $\bar{S}$ and $\bar{M}$ refer to the average values of the simulated and measured data, respectively.

The statistical performance metrics employed in this study (NRMSE, correlation coefficient r, and index of agreement d) are well established and extensively used in the literature for evaluating the agreement between simulated and observed datasets. Given their widespread adoption and rigorous documentation, their theoretical formulation and interpretation are not reiterated here. Instead, the reader is referred to the extensive body of published literature that comprehensively describes their mathematical basis, computation procedures, and performance benchmarks (Willmott, 1982; Jamieson et al., 1991; Blyth, 1994; Saad et al., 2014).

3. Results

3.1. Meteorological data during the growing seasons

Across the growing season (May–September, Fig. 5), decadal air temperatures in the three experimental years deviated from the long-term averages (1981–2021; LaMMA), with generally higher maximum temperatures, particularly during mid- and late summer (July–August). In 2021, Tmax values were mostly close to the long-term means, with increases generally within + 0.5 to + 1.5°C, mainly during the third decades of July and August. In contrast, 2022 exhibited consistently higher Tmax than the long-term reference, with positive anomalies frequently reaching + 2–3°C from June to August, while Tmin

values were also slightly higher (+ 1–2°C) during most decades. The 2023 growing season showed the highest thermal conditions overall, with both Tmin and Tmax exceeding long-term averages during several decades, particularly from late June to mid-August, with Tmax anomalies occasionally exceeding + 3–4°C. Cumulative precipitation showed high interannual variability relative to the long-term pattern. In 2021, rainfall was generally lower than the long-term average, with several decades receiving less than 1 mm of precipitation. Similarly, 2022 was characterized by extended dry periods during summer, with several consecutive decades recording 0–1 mm, despite isolated rainfall events in August and late September (up to ~ 50–120 mm in single decades). In contrast, 2023 displayed higher rainfall variability, with several decades exceeding the long-term cumulative precipitation, particularly in late spring and early autumn, when decadal totals reached 20–40 mm.

3.2. AquaCrop Calibration and Implementation

Simulated canopy cover values were in close agreement with field observations, as confirmed by the statistical performance indices (Table 3). The model slightly overestimated CC, with a simulated mean of 48.66% compared to an observed mean of 44.70%. Nevertheless, the correlation coefficient (r = 0.70) and the index of agreement (d = 0.82) indicate that the model effectively captured the temporal dynamics of canopy cover.

Table 3
Statistical indices of comparison of simulated vs. observed values of canopy cover (CC), total dry biomass (TDM), dry yield (Y) and soil water content (SWC) of rice in drip irrigation for the calibration phase, during 2022 growing season, under FARM water regime.

Parameter	Unit	Observation	Observed mean	Simulated mean	Diff. %	NRMSE[a]	r[b]	d[c]
CC	%	8	44.70	48.66	-3.97	0.34	0.70	0.82
TDM	t ha^{-1}	7	8.90	9.76	-0.86	0.24	0.94	0.95
Y	t ha^{-1}	2	3.95	4.04	-0.09			

[a]Normalized root mean square error; [b]Correlation coefficient; [c]Index of agreement of Willmott

The construction of the crop input file relied on the default settings of the model, complemented by

parameter calibrations reported in Wellens et al. (2022) and by the experimental findings presented in this study (Table 4).

Table 4
Conservative and non-conservative parameters of AquaCrop. Comparison between default values of rice as reported in the AquaCrop file version 6.1 Default.riceRICEGDD.CRO and calibrated values under the pedo-climatic condition of the Grosseto site.

Crop parameter	**Unit**	**Value**	
		Default	**Calibrated**
Canopy parameters:			
Initial canopy cover	%	0.06	0.06
Maximum canopy cover (CCx)	%	0.95	0.85
Canopy growth coefficient	% day^{-1}	0.12257	0.07249
Canopy decline coefficient	% GDD^{-1}	0.0933	0.150
Growing degree days:			
Base and upper limit temperature for GDD	°C	8; 30	8; 30
GDD from transplanting to recovered transplant	GDD	50	105
GDD from transplanting to flowering	GDD	1150	1046
GDD from transplanting to start senescence	GDD	1300	1588
GDD from transplanting to maturity	GDD	1900	2193
Length of the flowering stage	GDD	350	593
GDD from building-up of Harvest Index during yield formation	GDD	680	622
Root expansion:			
maximum effective rooting depth	m	0.50	0.50
minimum effective rooting depth	m	0.30	0.30
Harvest			
Reference Harvest Index	%	43	30
Water stress			
Soil water depletion factor for:			
canopy expansion (upper threshold)	-	0.00	0.25
canopy expansion (lower threshold)	-	0.40	0.60
stomatal closure	-	0.50	0.50
anticipated senescence	-	0.55	0.55

Crop parameter	Unit	Value	
		Default	Calibrated
Shape factor for water stress coefficient for:			
canopy expansion, stomatal closure, ant. senescence	-	3.0	3.0
Water efficiency			
Water productivity	g m^{-2}	19.0	21.0
Effect of water stress on yield during:			
Canopy expansion	-	none	small
Stomatal closure	-	strong	strong
† GDD, growing degree day(s)			

Figure 3 (a) illustrates the temporal evolution of canopy cover (%) as a function of days after planting (DAP), comparing experimentally observed data (points with error bars) with values simulated by the model (solid line) for the Caravaggio cultivar during the calibration year (2022). The trend clearly delineates the three main phases of crop development. During the initial stage (0–40 DAP), canopy cover increased gradually, reflecting crop emergence and early vegetative growth. In this period, CC ranged between 25–30%, indicating a limited interception of photosynthetically active radiation. A subsequent phase of rapid expansion (40–80 DAP) was observed, during which CC rose sharply to a maximum of approximately 75–80%, corresponding to the period of peak photosynthetic activity and full vegetative development. The narrow error bars indicate low variability, suggesting good agreement between measured and simulated data. In the final stage (> 100 DAP), CC declined progressively to around 20–25% at 140 DAP, marking the onset of leaf senescence and the consequent reduction of the photosynthetically active surface.

Overall, the AquaCrop model effectively reproduced the observed CC dynamics throughout the growing cycle, confirming its robustness in simulating crop growth processes and the reliability of the adopted calibration parameters.

The trend of total aboveground dry biomass accumulation (t ha^{-1}) over the crop growth cycle (2022), expressed as DAP, is also illustrated in Fig. 3b. Experimental data (orange square markers with error bars) are compared with values simulated by the AquaCrop model (solid line). As in the previous figure, the model demonstrates strong predictive performance, showing a satisfactory agreement between observed and simulated data throughout the entire growing period. The biomass accumulation pattern follows a typical sigmoidal curve characteristic of biological growth processes, comprising three main phases, *(i)* Initial phase (0–40 DAP): Biomass increases slowly, reflecting limited early vegetative growth associated with crop emergence and the development of initial photosynthetic structures. *(ii)* Rapid growth phase (40–110 DAP): A pronounced increase in biomass is observed, reaching values of

approximately 12 t ha⁻¹. This period corresponds to maximum photosynthetic activity and substantial leaf area expansion. *(iii)* Plateau phase (> 120 DAP): Biomass accumulation stabilizes around 15 t ha⁻¹, indicating the attainment of physiological maturity.

The error bars associated with the experimental data indicate moderate variability, consistent with field environmental and agronomic conditions. These findings confirm the model's reliability in simulating TDM dynamics, supporting its usefulness for assessing potential yields (as further discussed in Fig. 3) and for analyzing the effects of management or climatic scenarios on crop productivity. A comparison of simulated and observed yields (t ha⁻¹) from the AquaCrop model across three consecutive seasons (2021–2023) is shown in Fig. 6. Error bars represent intra-annual variability of field measurements. In 2021, the simulated yield (~ 3.0 t ha⁻¹) slightly exceeded the observed value (~ 2.7 t ha⁻¹), with wide error bars indicating strong variability likely linked to heterogeneous agronomic or climatic conditions. In 2022, simulated and observed yields (~ 3.5 t ha⁻¹) were comparable, though dispersion in observed data remained high, suggesting spatial or temporal heterogeneity in crop performance. The best agreement occurred in 2023, when both simulated and observed yields averaged ~ 4.0 t ha⁻¹, and error bars were minimal, reflecting more uniform field conditions and improved model accuracy.

Overall, AquaCrop showed robust predictive performance, particularly in years characterized by low inter-annual climatic variability, while deviations in earlier seasons were mainly due to variability in observed data rather than model bias. These results highlight the importance of reliable field datasets for model calibration and validation, and of accounting for environmental and management variability not explicitly represented in the model.

3.3 Water use and water footprint of irrigated rice

The analysis of water consumption and WF components across the three experimental years provides critical insights into the environmental sustainability of drip-irrigated rice cultivation in Mediterranean conditions (Fig. 4). Total crop water use (CWU) decreased progressively across the study period, from 7,289 m³ ha⁻¹ to 7,111 m³ ha⁻¹ and to 6,378 m³ ha⁻¹ in 2021, 2022 and 2023 respectively. This reduction was primarily attributable to declining irrigation requirements rather than changes in total water availability.

The green water component, representing precipitation-derived soil water consumed through transpiration, exhibited substantial inter-annual variability reflecting the contrasting climatic conditions. In the driest year (2021), with only 6 mm of rainfall during the growing cycle, green water contributed merely 59 m³ ha⁻¹ (0.8% of total CWU). In contrast, during 2022 and 2023, which received 263 mm and 162 mm of precipitation respectively, green water increased dramatically to 671 m³ ha⁻¹ (9.4%) and 698 m³ ha⁻¹ (10.9%). These values highlight the Mediterranean climate's characteristic rainfall deficit during the rice growing season, while demonstrating the system's capacity to effectively capture and utilize precipitation when available.

Blue water consumption, derived from irrigation applications, constituted the dominant fraction of total water use across all years. In 2021, irrigation volumes reached 6,890 $m^3\ ha^{-1}$ (94.5% of total CWU), decreasing substantially to 6,100 $m^3\ ha^{-1}$ (85.8%) in 2022 and 5,340 $m^3\ ha^{-1}$ (83.7%) in 2023. This progressive reduction reflects both improved precipitation patterns in later years and potentially enhanced irrigation efficiency through accumulated management experience. Notably, even in the driest year, total irrigation remained substantially below the 13,000–65,000 $m^3\ ha^{-1}$ range typically reported for continuously flooded rice systems in the same region (Arcieri & Ghinassi, 2020). The maximum irrigation volume observed (6,890 $m^3\ ha^{-1}$) represents approximately 47–53% of the lower bound of traditional flooding requirements, confirming the substantial water-saving potential of precision drip irrigation management. The WF, expressed per unit of grain production ($m^3\ t^{-1}$), exhibited substantial inter-annual variation inversely related to yield performance. Total WF decreased from 2,182 $m^3\ t^{-1}$ to 1,760 $m^3\ t^{-1}$ and to 1,603 $m^3\ t^{-1}$ in 2021, 2022 and 2023 respectively, representing a 27% improvement between the least and most favourable years. This progressive reduction occurred despite relatively stable total water consumption, indicating that yield improvements rather than water use reductions drove WF optimization across the study period. Blue WF constituted the dominant component, accounting for 92–95% of total WF across all years. Values ranged from 2,063 $m^3\ t^{-1}$ to 1,510 $m^3\ t^{-1}$ and to 1,342 $m^3\ t^{-1}$ in 2021, 2022 and 2023 respectively, demonstrates substantial improvement as yields increased from approximately 2.7 t ha^{-1} to 4.0 t ha^{-1}. These blue WF values are substantially lower than those reported for continuously flooded rice cultivation, where blue WF typically range from 2,200 to 2,800 $m^3\ t^{-1}$ in Mediterranean climates (Chapagain & Hoekstra, 2011). The blue WF in 2023 (1,342 $m^3\ t^{-1}$) represents a reduction of approximately 40–52% compared to conventional flooding benchmarks, confirming the enhanced environmental performance of drip irrigation, despite the lower absolute yields compared to traditional methods. Green WF increased from 18 $m^3\ t^{-1}$ to 166 $m^3\ t^{-1}$ and to 175 $m^3\ t^{-1}$ in 2021, 2022 and 2023 respectively. While green WF contributed only 0.8–10.9% of total WF, its proportional increase in wetter years demonstrates the system's capacity to capitalize on precipitation when temporally aligned with crop water demand, partially offsetting irrigation requirements without compromising yield stability. Finally, Grey WF represented 4.7–5.3% of total WF, indicating that current fertilization practices maintain acceptable environmental performance with relatively minor contribution to overall WF.

4. Discussion

The AquaCrop model demonstrated robust predictive performance throughout the calibration and validation phases, confirming its reliability for simulating rice growth under drip irrigation conditions in Mediterranean environments. The alignment between simulated and observed data for canopy cover, total dry biomass, and grain yield showed that the model successfully captured the key physiological processes governing crop development under non-flooded conditions. These results align with recent AquaCrop validation studies for rice conducted globally. Maniruzzaman et al. (2015) achieved prediction errors for grain yield between 5.55 and 11.54% across different irrigation regimes in Bangladesh, while Mostafa et al. (2023) reported excellent model performance in optimizing irrigation strategies in China. Similarly, Phoeurn et al. (2024) obtained Willmott's index values of 1.0 with minimal root mean square

errors, demonstrating high model accuracy under alternate wetting and drying conditions. The capacity of AquaCrop to reliably simulate crop responses under water-limited conditions makes it especially valuable for Mediterranean agriculture, where optimizing irrigation is critical for sustainability.

The multi-year evaluation provided clear evidence that drip irrigation sustained rice production under Mediterranean conditions while substantially reducing pressure on freshwater resources. Grain yields observed in this study fall within the range commonly reported for non-flooded rice systems globally. Akbar et al. (2025a) documented yields of 3.4 t ha^{-1} for drip-irrigated rice in Pakistan, with water productivity improvements exceeding 20% compared to conventional flooding. Arif et al. (2024) similarly reported that subsurface drip irrigation in aerobic rice systems achieved water savings above 40% while maintaining acceptable productivity. These findings are consistent with trials conducted under arid Mediterranean conditions, where Mousa et al. (2024) observed that diverse rice genotypes maintained stable yields under substantially reduced irrigation regimes, with water use efficiency improvements ranging from 25 to 45%. Soltani et al. (2024) further confirmed that aerobic rice systems in Iran's semi-arid regions reduced irrigation requirements by approximately half compared to flooded systems while preserving economic viability.

The yields observed in this study were lower than those normally achieved in northern Italy's Po Valley, where flooded rice systems typically produce 6.0 to 7.5 t ha^{-1} (Ranghetti & Boschetti, 2022). However, this comparison must be contextualized. The Tuscany environment differs fundamentally in temperature regimes, soil characteristics, rooting depth potential and land preparation history. More importantly, drip-irrigated rice represents an agronomically novel system that lacks the century-long optimization characterizing northern Italian paddy landscapes. Rather than interpreting the yield gap as an inefficiency, the results demonstrate that drip irrigation enabled stable production under water-limited conditions where traditional flooding would be environmentally unsustainable or economically impractical. This stability across three meteorologically contrasting years demonstrates the system's capacity to buffer hydro-climatic variability. Similar trends have been reported in aerobic rice trials across Asia and Australia, where agronomic adaptation to local patterns initially required transition periods but ultimately enhanced long-term resilience (Fukai & Mitchell, 2022). The consistency of field observations across contrasting seasons confirmed that micro-irrigated rice maintained physiological activity without standing water, provided soil moisture remained above critical thresholds. This finding is coherent with emerging research demonstrating that rice does not intrinsically require submersion if soil water balance is adequately managed (Farooq et al., 2023; Fukai & Mitchell, 2022).

Canopy dynamics followed patterns typical of well-functioning rice, with leaf area development progressing steadily through vegetative and reproductive phases despite the absence of a water layer. The observed coherence between simulated and measured CC throughout multiple growth stages indicated that the irrigation system sustained transpiration without inducing severe water stress. This behavior aligned with studies in aerobic rice systems where crops maintained comparable canopy trajectories to submerged rice when soil-water balance was stabilized through high-frequency irrigation (Froes de Borja Reis et al., 2018; Çolak, 2021;). Biomass accumulation likewise progressed continuously

throughout the growing cycle, showing values consistent with reports for non-flooded rice under controlled moisture conditions. While small deviations near maturity were expected—given the challenges that crop models face in representing senescence and assimilating remobilization dynamics—the multi-year consistency strengthened the interpretation that the drip irrigation system provided adequate conditions for sustained plant growth.

One of the most significant findings was the transformation of the seasonal water balance induced by drip irrigation. Traditional flooded rice is characterized by substantial unproductive water losses—including percolation, seepage, and surface evaporation—often accounting for more water than transpiration itself (Chapagain & Hoekstra, 2011). The drip-irrigated system-maintained soil moisture within a controlled range, applying water only when required, thereby sharply reducing non-productive evapotranspiration components. The irrigation volumes observed in this study were consistent with documented reductions in water demand for drip- or sprinkler-based rice systems reported globally. Recent literature confirms substantial water savings potential.Akbar et al. (2025b) reported water productivity improvements exceeding 40% for drip-irrigated rice compared to flood irrigation, while the comprehensive meta-analysis by Sounon Orou et al. (2025), synthesizing 573 observations from 56 studies, found that aerobic rice systems and alternate wetting-drying techniques achieved water savings up to 25% improvement in WF compared to continuous flooding while maintaining economically viable yields.

The WF analysis provided an integrated measure of freshwater appropriation across the three water components. Rice is traditionally associated with elevated WF values, especially in its blue component, due to the structural requirement to maintain standing water throughout much of the growing season. Global assessments consistently indicate blue WF for submerged rice frequently exceeds 1200 to 2500 $m^3\ t^{-1}$ (Chapagain & Hoekstra, 2011; Mekonnen & Hoekstra, 2011). The values obtained in this study, particularly the dominance of blue water in determining total WF, aligned closely with findings from Wu et al. (2022), who documented WF reductions from 1000 $m^3\ t^{-1}$ under flood irrigation to 910 $m^3\ t^{-1}$ under water-saving irrigation systems. Their analysis revealed shifts in WF composition, with blue water contribution decreasing from 17% to 10% (– 47% for the blue water) of total WF while green water utilization improved correspondingly. By eliminating the need for continuous ponding, the drip-irrigated system substantially reduced irrigation withdrawals per unit of grain produced.

The improved efficiency translated into stable blue WF values across climatically contrasting years, demonstrating limited sensitivity to interannual rainfall variability. This stability contrasted sharply with flooded systems, whose WF exhibits high dependence on seasonal climatic patterns. The proportional increase in green WF contribution reflected more efficient rainfall infiltration directly into the root zone rather than contributing to surface water layers subject to high evaporative losses. The grey WF component remained relatively low due to minimal drainage volumes and reduced nutrient transport pathways, consistent with studies documenting enhanced nitrogen use efficiency and lower nitrate leaching under precision fertigation systems (Fan et al., 2020). These findings suggest that transitioning

from flooded to drip-irrigated rice cultivation offers substantial environmental benefits beyond water conservation alone.

An indirect but environmentally significant implication of the water balance transformation relates to greenhouse gas emissions. Flooded rice cultivation is recognized as a major source of atmospheric methane due to anaerobic soil conditions that prevail under continuous submersion, accounting for approximately 8 to 11% of global agricultural greenhouse gas emissions (Edenhofer, 2015; Saunois et al., 2020). By maintaining soils in predominantly unsaturated states, drip irrigation inherently limits the biogeochemical pathways responsible for methanogenesis. Likewise, Islam et al. (2020) reported that alternate wetting and drying irrigation reduced total greenhouse gas emissions by 51% compared to continuous flooding, with substantial decreases in methane fluxes. Similarly, comparative studies of aerobic versus flooded rice systems documented methane emission reductions exceeding 50%, though modest increases in nitrous oxide emissions were observed (Anapalli et al., 2023). On a CO_2-equivalent basis, the net climate benefit remains strongly positive, as the reduction in methane far outweighs the increase in nitrous oxide due to their differing global warming potentials.

The multi-year stability of production despite highly variable climatic conditions represents a critical advantage for Mediterranean agriculture facing increasing climate uncertainty. The capacity to maintain acceptable yields across seasons characterized by extreme drought, above-average temperatures, and irregular precipitation patterns demonstrated the buffering potential of precision irrigation management. This resilience contrasts with the inherent vulnerability of flooded systems, which require stable water availability throughout the season and become increasingly difficult to sustain as water resources become more variable and contested. Sounon Orou et al. (2025) emphasized that integration of appropriate agronomic practices with water management technologies led to similar yields across continuous flooding, soil saturation, and moderate alternate wetting and drying treatments, with aerobic systems showing the most stable performance across environmental gradients. Their meta-analysis further revealed that short-cycle varieties under water-saving irrigation-maintained yield stability superior to medium- and long-cycle varieties, which experienced greater sensitivity to water deficit conditions.

Taken together, these findings suggest that drip-irrigated rice represents a viable strategy for sustaining rice cultivation in water-limited Mediterranean landscapes while addressing multiple sustainability dimensions simultaneously. The system maintained stable yields across meteorologically variable seasons while substantially reducing overall water consumption compared to traditional flooding. By shifting the water balance in favor of productive transpiration over unproductive evaporation, the system lowered the blue WF a critical advantage given the intensifying competition for freshwater resources under climate change. The evidence accumulated across three contrasting growing seasons demonstrated that rice cultivation in central Italy and similar Mediterranean environments can be fundamentally redesigned around precision water management principles, moving decisively away from the traditional paradigm of continuous flooding. This transition, supported by converging evidence from global research and validated through the WF framework adopted in this study, indicates that rice can be successfully re-integrated into Mediterranean cropping systems in a substantially more resource-

efficient and environmentally compatible form. The validation of AquaCrop as a reliable tool for simulating drip-irrigated rice further strengthens the foundation for expanding this approach, providing a robust platform for scenario analysis, irrigation scheduling optimization, and adaptation planning under future climate conditions. Recent comprehensive reviews emphasize the centrality of water-saving technologies for future rice sustainability (Bin Rahman & Zhang, 2023) while detailed analyses of aerobic rice systems identify cultivar selection, nitrogen management optimization, and precision irrigation scheduling as key determinants of success (Fukai & Mitchell, 2022). The convergence of agronomic innovation, validated modeling tools, and environmental necessity provides a compelling rationale for transitioning Mediterranean rice cultivation toward systems that align productivity with long-term resource availability and ecological sustainability.

5. Conclusion

The results of this study demonstrate that climate change, characterized by rising temperatures and irregular precipitation patterns, is expected to affect rice production in Tuscany significantly. Despite the prevalence of traditional flooding, micro-irrigation strategies could achieve yields comparable to flooded controls, demonstrating a significant opportunity for optimizing water resource management. The AquaCrop model demonstrates high reliability in simulating rice growth and predicting yield across different irrigation strategies and climatic conditions. The analysis of WF indicated that the blue water component had the greatest influence on total WF. Shifting from traditional flooded systems to more efficient irrigation significantly reduced WF, thus highlighting the environmental benefits of adopting water-saving practices. However, the results are subject to uncertainties related to future climate projections, the reliance on a single crop model, and the limited geographic scope of the study. Economic aspects of climate change adaptation were also not fully addressed. To derive more robust conclusions, further research is needed using multiple crop models, broader geographic coverage, and integration of economic and practical factors. Despite these limitations, the findings provide valuable insights for policymakers and farmers, offering guidance for developing climate change adaptation and mitigation strategies that enhance resilience and promote more sustainable rice production in Tuscany and regions with similar agro-climatic conditions.

Declarations

CRediT authorship contribution statement

Filiberto Altobelli: Writing – review & editing, Supervision, Project administration, Conceptualization. **Pasquale Garofalo**: Writing – original draft, Software, Methodology, Formal analysis, Conceptualization. **Andrea Martelli**: Writing – review & editing, Conceptualization. **Itzel Inti Maria Donati**: Writing – review & editing, Writing – original draft, Formal analysis, Conceptualization. **Davide Rapinesi**: Writing – review & editing. **Stefano Monaco**: Writing – review & editing. **Leonardo Verdi**: Writing – original draft. **Anna Dalla Marta**: Writing – original draft.

Declaration of Competing Interest

The authors declare that they have no known competing financial interests or personal relationships that could have appeared to influence the work reported in this paper.

Author Contribution

F. A.: Writing – review & editing, Supervision, Project administration, Conceptualization. P.G.: Writing – original draft, Software, Methodology, Formal analysis, Conceptualization. A.M.: Writing – review & editing, Conceptualization. I.I.M.D.: Writing – review & editing, Writing – original draft, Formal analysis, Conceptualization. D.R.: Writing – review & editing. S.M.: Writing – review & editing. L.V.: Writing – original draft. A.D.M: Writing – original draft.

Acknowledgement

We gratefully acknowledge Ente Terre Regionali Toscane, a non-economic public body of the Tuscany Region, established under Regional Law 80/2012 (formerly the Alberese Agricultural Estate), dedicated to enhancing the regional agricultural and forestry heritage. It manages public land, promotes sustainability, research, and legality, and oversees the Regional Agricultural and Forestry Heritage, and Fattoria Poggetti Vecchi società semplice agricola for their valuable support during the field experimental campaign conducted in the Province of Grosseto, Tuscany, Italy.

Data Availability

The authors declare that they have no known competing financial interests or personal relationships that could have appeared to influence the work reported in this paper.

References

1. Abi Saab MT, Todorovic M, Albrizio R (2015) Comparing aquaCrop and cropSyst models in simulating barley growth and yield under different water and nitrogen regimes: Does calibration year influence the performance of crop growth models? Agric Water Manage 147:21–33. https://doi.org/10.1016/j.agwat.2014.08.001
2. Akbar G, Islam Z, Khalil SH, Wali Z (2025a) Enhancing the irrigation water productivity of rice farming: A study on sowing and irrigation practices in Pakistan. Irrig Sci 74(1):332–341. https://doi.org/https://doi.org/10.1002/ird.2981
3. Akbar G, Islam Z, Khalil SH, Wali Z (2025b) Enhancing the irrigation water productivity of rice farming: A study on sowing and irrigation practices in Pakistan. Irrig Sci 74(1):332–341. https://doi.org/https://doi.org/10.1002/ird.2981

4. Allen RG, Pruitt WO, Wright JL, Howell TA, Ventura F, Snyder R, Itenfisu D, Steduto P, Berengena J, Yrisarry JB, Smith M, Pereira LS, Raes D, Perrier A, Alves I, Walter I, Elliott R (2006) A recommendation on standardized surface resistance for hourly calculation of reference ETo by the FAO56 Penman-Monteith method. Agric Water Manage 81(1–2):1–22. https://doi.org/10.1016/j.agwat.2005.03.007
5. Altobelli F, Cimino O, Natali F, Orlandini S, Gitz V, Meybeck A, Dalla Marta A (2018) Irrigated farming systems: using the water footprint as an indicator of environmental, social and economic sustainability. J Agricultural Sci 156(5):711–722. https://doi.org/DOI: 10.1017/S002185961800062X
6. Anapalli SS, Pinnamaneni SR, Reddy KN, Wagle P, Ashworth AJ (2023) Eddy covariance assessment of alternate wetting and drying floodwater management on rice methane emissions. Heliyon 9(4). https://doi.org/10.1016/j.heliyon.2023.e14696
7. Arcieri M, Ghinassi G (2020) Rice cultivation in Italy under the threat of climatic change: Trends, technologies and research gaps. In *Irrigation and Drainage* (Vol. 69, Number 4, pp. 517–530). John Wiley and Sons Ltd. https://doi.org/10.1002/ird.2472
8. Arif C, Saptomo SK, Setiawan BI, Taufik M, Suwarno WB, Nugroho BDA, Mizoguchi M (2024) Water saving rice cultivation using sheet-pipe subsurface irrigation. Heliyon 10(10). https://doi.org/10.1016/j.heliyon.2024.e30799
9. Bin Rahman ANMR, Zhang J (2023) Trends in rice research: 2030 and beyond. In *Food and Energy Security* (Vol. 12, Number 2). John Wiley and Sons Inc. https://doi.org/10.1002/fes3.390
10. Blyth S (1994) Karl Pearson and the Correlation Curve. Int Stat Rev / Revue Int de Statistique 62(3):393–403. https://doi.org/10.2307/1403769
11. Bouman BAM, Lampayan RM, Tuong TP (2007) Water management in irrigated rice: coping with water scarcity. International Rice Research Institute
12. Chapagain AK, Hoekstra AY (2011) The blue, green and grey water footprint of rice from production and consumption perspectives. Ecol Econ 70(4):749–758. https://doi.org/https://doi.org/10.1016/j.ecolecon.2010.11.012
13. Çolak Y (2021) Comparison of aerobic rice cultivation using drip systems with conventional flooding. J Agricultural Sci 159:1–13. https://doi.org/10.1017/S0021859621000824
14. Datta A, Ullah H, Ferdous Z (2017) Water Management in Rice. In B. S. Chauhan, K. Jabran, & G. Mahajan (Eds.), *Rice Production Worldwide* (pp. 255–277). Springer International Publishing. https://doi.org/10.1007/978-3-319-47516-5_11
15. Edenhofer O (2015) Climate change 2014: mitigation of climate change : Working Group III contribution to the Fifth assessment report of the Intergovernmental Panel on Climate Change. Cambridge University Press
16. Farooq MS, Fatima H, Rehman OU, Yousuf M, Kalsoom R, Fiaz S, Khan MR, Uzair M, Huo S (2023) Major challenges in widespread adaptation of aerobic rice system and potential opportunities for

future sustainability. South Afr J Bot (Vol 159:231–251. https://doi.org/10.1016/j.sajb.2023.06.017. Elsevier B.V

17. Froes deB, Reis A, de Estevam Munhoz R, Cocco Lago B, Trivelin PC, Linquist B, Favarin JL (2018) Aerobic rice system improves water productivity, nitrogen recovery and crop performance in Brazilian weathered lowland soil. Field Crops Res 218:59–68. https://doi.org/10.1016/j.fcr.2018.01.002
18. Fukai S, Mitchell J (2022) Factors determining water use efficiency in aerobic rice. In *Crop and Environment* (Vol. 1, Number 1, pp. 24–40). Elsevier B.V. https://doi.org/10.1016/j.crope.2022.03.008
19. Heng LK, Hsiao T, Evett S, Howell T, Steduto P (2009a) Validating the FAO aquacrop model for irrigated and water defi cient field maize. Agron J 101(3):488–498. https://doi.org/10.2134/agronj2008.0029xs
20. Heng LK, Hsiao T, Evett S, Howell T, Steduto P (2009b) Validating the FAO aquacrop model for irrigated and water defi cient field maize. Agron J 101(3):488–498. https://doi.org/10.2134/agronj2008.0029xs
21. Islam SF, ul, Sander BO, Quilty JR, de Neergaard A, van Groenigen JW, Jensen LS (2020) Mitigation of greenhouse gas emissions and reduced irrigation water use in rice production through water-saving irrigation scheduling, reduced tillage and fertiliser application strategies. *Science of the Total Environment*, *739*. https://doi.org/10.1016/j.scitotenv.2020.140215
22. Jacovides CP, Kontoyiannis H (1995) Statistical procedures for the evaluation of evapotranspiration computing models. Agric Water Manage 27(3):365–371. https://doi.org/https://doi.org/10.1016/0378-3774(95)01152-9
23. Jamieson PD, Porter JR, Wilson DR (1991) A test of the computer simulation model ARCWHEAT1 on wheat crops grown in New Zealand. Field Crops Res 27(4):337–350. https://doi.org/https://doi.org/10.1016/0378-4290(91)90040-3
24. Katerji N, Campi P, Mastrorilli M (2013) Productivity, evapotranspiration, and water use efficiency of corn and tomato crops simulated by AquaCrop under contrasting water stress conditions in the Mediterranean region. Agric Water Manage 130:14–26. https://doi.org/10.1016/j.agwat.2013.08.005
25. Kitilu MJF, Nyomora AMS, Charles J (2019) Moisture requirement and water productivity of selected rainfed rice varieties grown under controlled water environment in Ifakara, Tanzania. J Cereals Oilseeds 10(1):1–15. https://doi.org/10.5897/jco2018.0188
26. Lamastra L, Suciu NA, Novelli E, Trevisan M (2014) A new approach to assessing the water footprint of wine: An Italian case study. Sci Total Environ 490:748–756
27. Macchia M, Ceccarini L, Molfetta I, Cioni PL, Flamini G (2013) Studies on saffron (Crocus sativus L.) from Tuscan Maremma (Italy): Effects of geographical origin, cultivation environment and drying method on volatile emission. Int J Food Sci Technol 48(11):2370–2375. https://doi.org/10.1111/ijfs.12227

28. Mahmoud SH, Ati AS, Majeed SS (2024) Calculating Water Productivity Using the Portal WaPOR. *IOP Conference Series: Earth and Environmental Science*, *1371*(8). https://doi.org/10.1088/1755-1315/1371/8/082039
29. Mallareddy M, Thirumalaikumar R, Balasubramanian P, Naseeruddin R, Nithya N, Mariadoss A, Eazhilkrishna N, Choudhary AK, Deiveegan M, Subramanian E, Padmaja B, Vijayakumar S (2023) Maximizing Water Use Efficiency in Rice Farming: A Comprehensive Review of Innovative Irrigation Management Technologies. In *Water (Switzerland)* (Vol. 15, Number 10). MDPI. https://doi.org/10.3390/w15101802
30. Maniruzzaman M, Talukder MSU, Khan MH, Biswas JC, Nemes A (2015) Validation of the AquaCrop model for irrigated rice production under varied water regimes in Bangladesh. Agric Water Manage 159:331–340. https://doi.org/10.1016/j.agwat.2015.06.022
31. Martelli A, Rapinesi D, Verdi L, Donati IIM, Marta D, A., Altobelli F (2025) Smart irrigation for management of processing tomato: a machine learning approach. Irrig Sci 43(6):1407–1424. https://doi.org/10.1007/s00271-024-00993-9
32. Mekonnen MM, Hoekstra AY (2011) *The green, blue and grey water footprint of crops and derived crop products*. https://doi.org/10.5194/hessd-8-763-2011
33. Mostafa M, Luo W, Zou J, Salem A (2023) Optimizing Rice Irrigation Strategies to Maximize Water Productivity: A Simulation Study Using AquaCrop Model for the Yanyun Irrigation District, Yangzhou, China. Earth (Switzerland) 4(3):445–460. https://doi.org/10.3390/earth4030024
34. Mousa AMA, Ali AMA-G, Omar AEA, Alharbi K, El-Moneim DA, Mansour E, Elmorsy RS (2024) A. Physiological, Agronomic, and Grain Quality Responses of Diverse Rice Genotypes to Various Irrigation Regimes under Aerobic Cultivation Conditions. *Life*, *14*. https://api.semanticscholar.org/CorpusID:268404063
35. Nash JE, Sutcliffe JV (1970) River flow forecasting through conceptual models part I — A discussion of principles. J Hydrol 10(3):282–290. https://doi.org/https://doi.org/10.1016/0022-1694(70)90255-6
36. Phoeurn CA, Degré A, Oeurng C, Ket P (2024) Evaluating the impact of climate change on yield and water use efficiency of different dry-season rice varieties cultivated under conventional and alternate wetting and drying conditions. Environ Monit Assess 196(12):1190
37. Ponce De León MA, Bailey BN (2019) *Evaluating the use of Beer's law for estimating light interception in canopy architectures with varying heterogeneity and anisotropy*
38. Raes D, Steduto P, Hsiao TC, Fereres E (2009) Aquacrop-The FAO crop model to simulate yield response to water: II. main algorithms and software description. Agron J 101(3):438–447. https://doi.org/10.2134/agronj2008.0140s
39. Ranghetti L, Boschetti M (2022) Updated trends of water management practice in the Italian rice paddies from remotely sensed imagery. Eur J Remote Sens 55(1):1–9. https://doi.org/10.1080/22797254.2021.2002726

40. Rinaldi M (n.d.). *Processing tomatoes under different irrigation regimes in Southern Italy: Agronomic and economic assessments in a simulation case study*. Retrieved https://www.researchgate.net/publication/283299918
41. Rinaldi M, Garofalo P (2011) Radiation-use efficiency of irrigated biomass sorghum in a Mediterranean environment. Crop Pasture Sci 62(10):830–839
42. Saad II, Saha SB, Thomas G (2014) Hypothesis The RAS subfamily Evolution-tracing evolution for its utmost exploitation. Print) Bioinformation 10(5):293.
43. Sasmita P, Agustiani N, Margaret S, Ardhiyanti D, S., Nugraha Y (n.d.). *Drip Irrigation Technology Performance on Rice Cultivation*. https://doi.org/10.23960/jtep-l.v11.i1.130-145
44. Saunois M, Stavert R, Poulter A, Bousquet B, Canadell PG, Jackson JB, Raymond RA, Dlugokencky PJ, Houweling E, Patra SK, Ciais P, Arora PK, Bastviken V, Bergamaschi D, Blake PR, Brailsford D, Bruhwiler G, Carlson LM, Carrol K, Zhuang M, Q (2020) The global methane budget 2000–2017. Earth Syst Sci Data 12(3):1561–1623. https://doi.org/10.5194/essd-12-1561-2020
45. Soltani A, Jafarnode S, Zeinali E, Gherekhloo J, Torabi B (2024) Assessing aerobic rice systems for saving irrigation water and paddy yield at regional scale. Paddy Water Environ 22(2):271–284. https://doi.org/10.1007/s10333-023-00966-2
46. Sounon Orou BZ, Adjogboto A, Zakari S, Tovihoudji PG, Akponikpè PBI, Vanclooster M (2025) Improving rice yield and water productivity in lowland rice systems: A global meta-analysis exploring the synergy of agro-ecological practices and water management technologies. In *Irrigation and Drainage* (Vol. 74, Number 1, pp. 471–489). John Wiley and Sons Ltd. https://doi.org/10.1002/ird.3005
47. Steduto P, Hsiao TC, Fereres E, Raes D (n.d.). *Crop yield response to water*
48. Steduto P, Hsiao TC, Raes D, Fereres E (2009) Aquacrop-the FAO crop model to simulate yield response to water: I. concepts and underlying principles. Agron J 101(3):426–437. https://doi.org/10.2134/agronj2008.0139s
49. *The dimensions of water productivity*. (n.d.)
50. Wellens J, Raes D, Fereres E, Diels J, Coppye C, Adiele JG, Ezui KSG, Becerra LA, Selvaraj MG, Dercon G, Heng LK (2022) Calibration and validation of the FAO AquaCrop water productivity model for cassava (Manihot esculenta Crantz). *Agricultural Water Management*, *263*. https://doi.org/10.1016/j.agwat.2022.107491
51. Willmott CJ (1982) *Some Comments on the Evaluation of Model Performance*
52. Wu M, Li Y, Xiao J, Guo X, Cao X (2022) Blue, green, and grey water footprints assessment for paddy irrigation-drainage system. J Environ Manage 302:114116. https://doi.org/https://doi.org/10.1016/j.jenvman.2021.114116

Figures

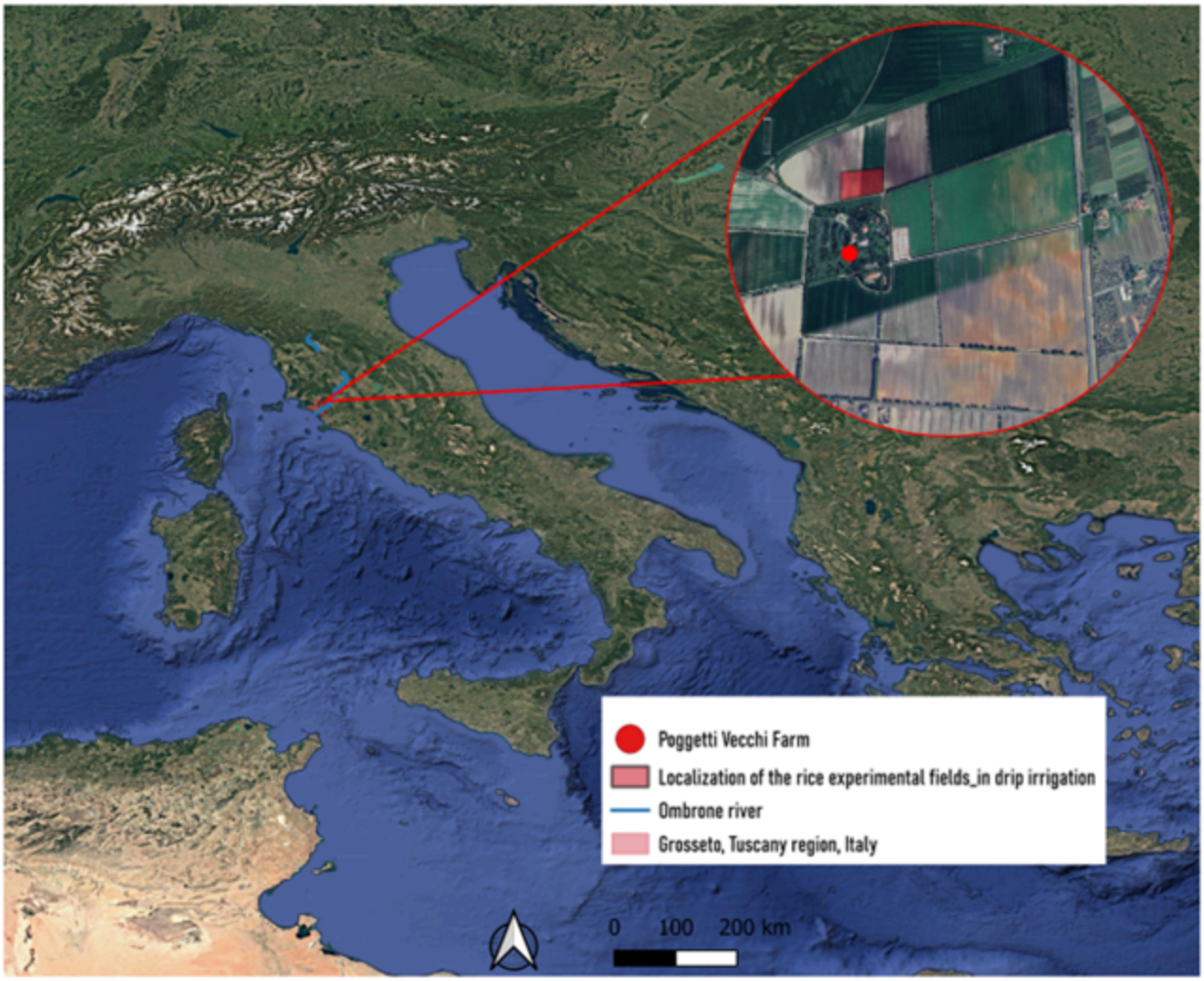


Figure 1

Localization of the experimental rice plots, Grosseto, Tuscany.

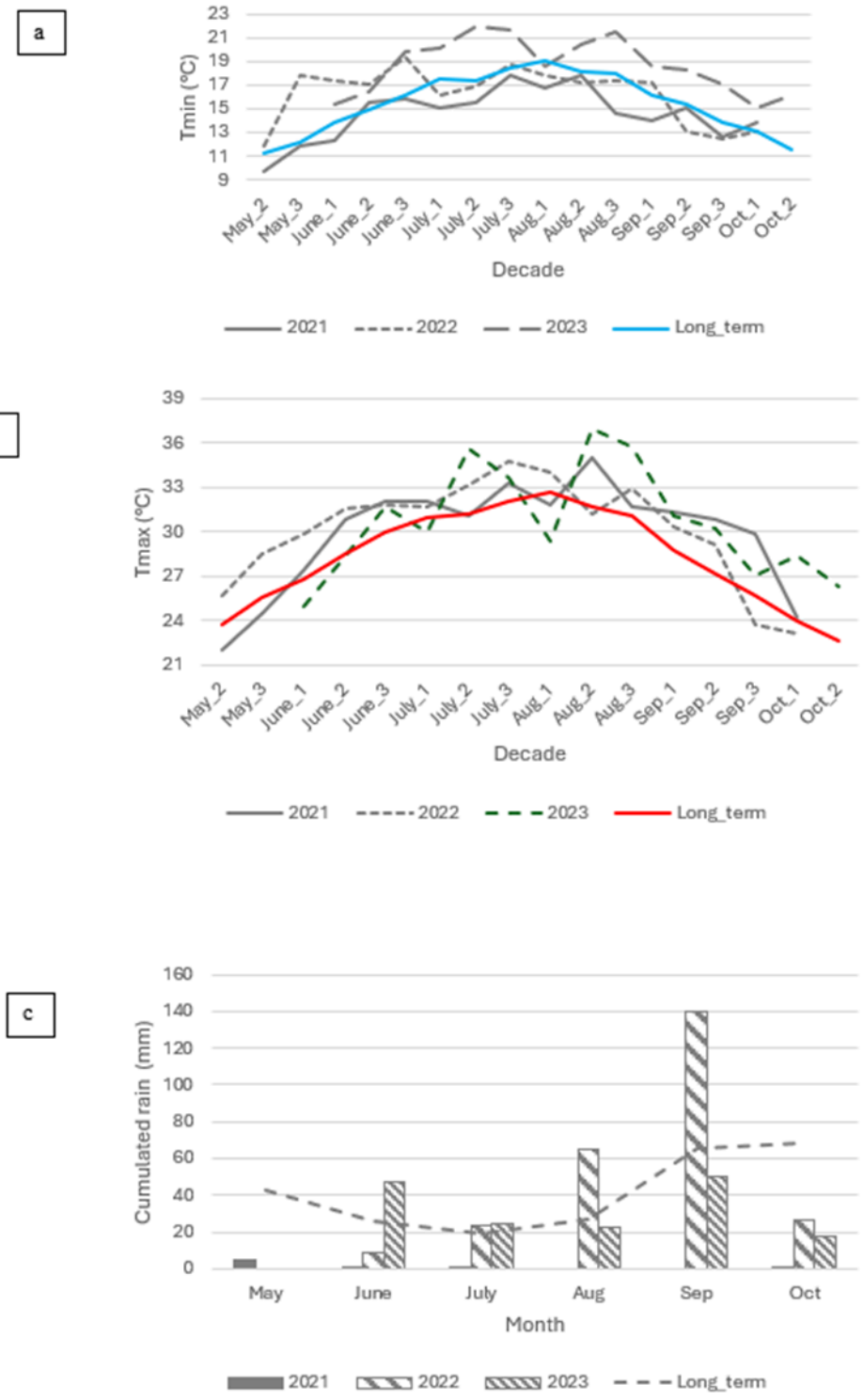


Figure 2

Decadal averages of maximum air temperature (a), minimum air temperature (b), and cumulative precipitation (c) in the experimental area during the three growing seasons, compared with the long-term climatological average.

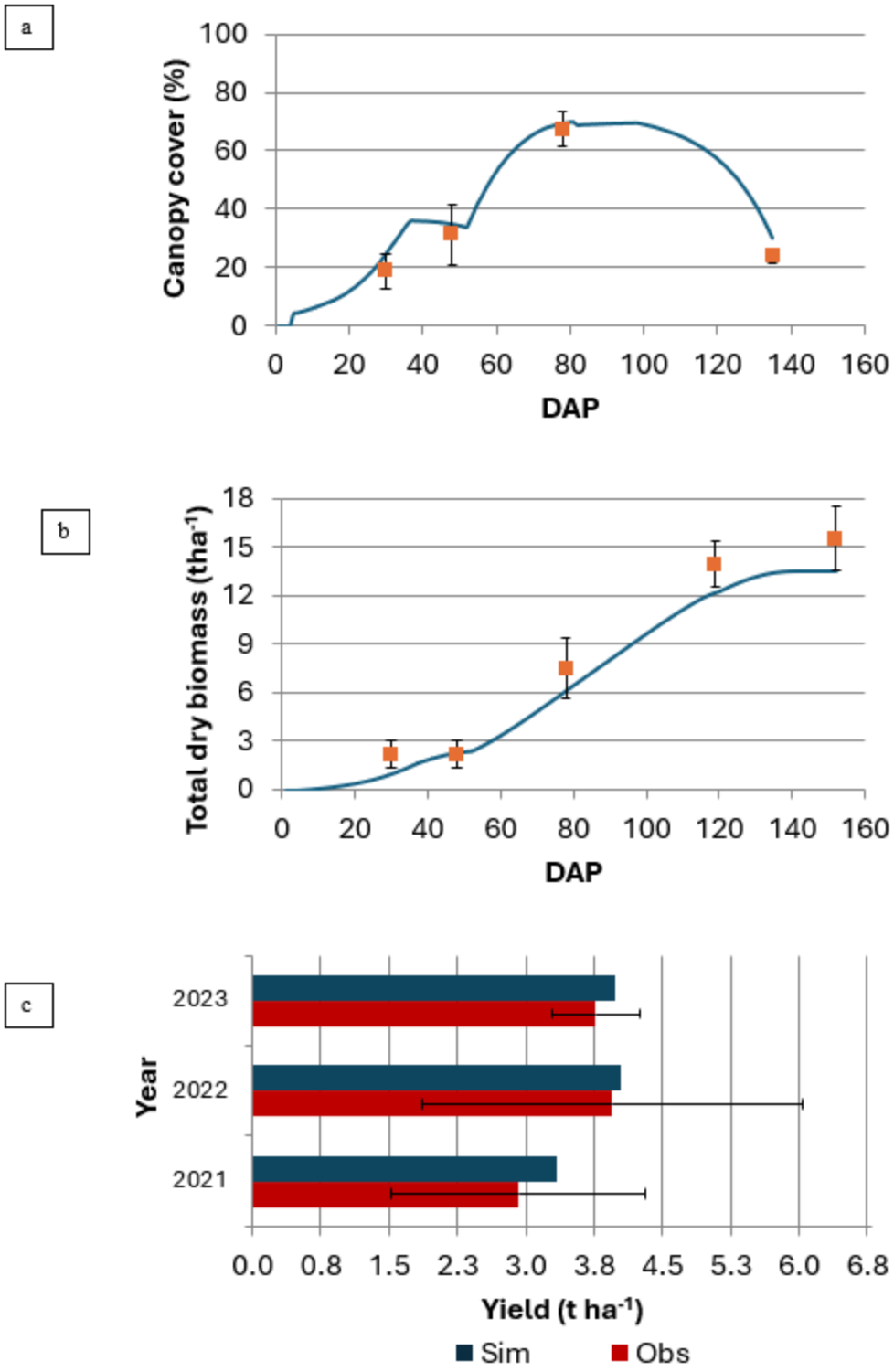


Figure 3

Comparison between simulated and observed data of canopy cover (CC) – a - and total dry biomass (TDM) -b- for the calibration process and yield for the experimental years (c). Bars indicate the standard deviation. DAP= days after planting

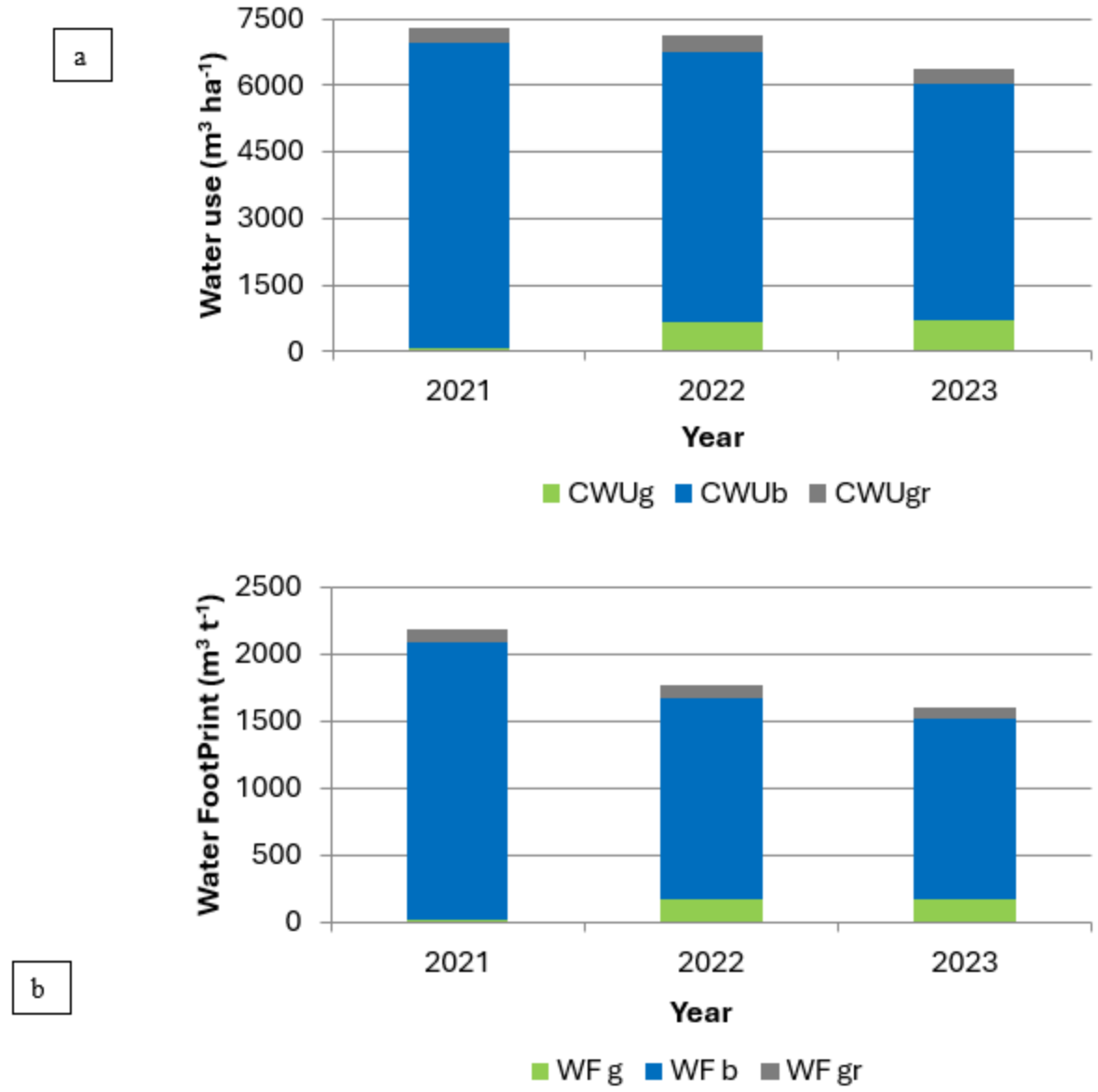


Figure 4

Crop water use (CWU; a) and Water Footprint (WF; b) as resulting from the green (g), blue (b) and grey (g) components derived from the simulation outputs for the three experimental years.